ELSEVIER

Chemical Engineering Journal 140 (2008) 183–192

Chemical Engineering Journal

www.elsevier.com/locate/cej

Enhanced fluoride removal from drinking water by magnesia-amended activated alumina granules

Shihabudheen M. Maliyekkal, Sanjay Shukla, Ligy Philip *, Indumathi M. Nambi

Department of Civil Engineering, EWRE Division, Indian Institute of Technology-Madras, Chennai 600036, India

Received 12 April 2007; received in revised form 19 September 2007; accepted 24 September 2007

Abstract

This paper describes the fluoride removal potential of a novel sorbent, magnesia-amended activated alumina (MAAA) from drinking water. MAAA, prepared by calcining magnesium hydroxide impregnated alumina at 450 °C has shown high fluoride sorption potential than activated alumina from drinking water. Batch sorption studies were performed as a function of contact time, pH, initial fluoride concentration, and adsorbent dose. Studies were also performed to understand the effect of various other co-existing ions present in real ground water samples. X-ray powder diffraction (XRD), scanning electron microscope (SEM), energy dispersive X-ray (EDAX) and a gas adsorption porosimetry analyses were used to characterize the physicochemical properties of MAAA. More than 95% removal of fluoride (10 mg l^{-1}) was achieved within 3 h of contact time at neutral pH. Sorption of fluoride onto MAAA was found to be pH dependant and a decrease in sorption was observed at higher pHs. Among the kinetic models tested, pseudo-second-order model fitted the kinetic data well, suggesting the chemisorption mechanism. Among the various isotherm model tested, Sips model predicted the data well. The maximum sorption capacity of fluoride deduced from Sips equation was 10.12 mg g^{-1}. Most of the co-existing ions studied have negligible effect on fluoride sorption by MAAA. However, higher concentrations of bicarbonate and sulfate have reduced the fluoride sorption capacity.

Keywords: Sorption; Fluoride; Drinking water; Magnesia-amended activated alumina; Kinetics

1. Introduction

Low concentrations of fluoride in drinking water have been considered beneficial to prevent dental carries. But scientists are now debating on the health benefits of fluoride even at low concentrations. It has long been known that chronic intake of excessive fluoride (>1 mg l^{-1}) can lead to severe dental and skeletal fluorosis. It not only affects teeth and skeleton, but its accumulation over a long period can also lead to change in the DNA structure [1,2].

Consumption of ground water containing high levels of fluoride concentration is one of the major exposure mechanism to the public in India and in many other parts of the world. Drinking water sources in India have fluoride concentration as high as 30 mg l^{-1}. According to World Health Organization (WHO) guidelines, the fluoride concentration in drinking water should not exceed 1.5 mg l^{-1} [3]. However, this guideline value of fluoride is not universal.

Fluoride removal from drinking water can be achieved by chemical precipitation, adsorption onto activated alumina, membrane process and ion exchange. Among these processes, membrane and ion exchange processes are not very common due to its high installation and maintenance cost. Other two methods are very common in India, especially chemical precipitation by addition of alum and lime mixture into fluoride-contaminated water (Nalagonda technique). However, the associated problems like generation of acid/alkali water, residual aluminium and soluble aluminium fluoride complexes, generation of sludges, and relatively higher residual fluoride concentrations are of major concern [4–6].

Adsorption onto solid surface is a simple, versatile and appropriate process for treating drinking water system, especially for small communities. Adsorption technique is considered as economical and can remove ions over a wide pH range and to a lower residual concentration than precipitation. Activated alumina is one of the best available and generally used sorbent for defluoridation of drinking water [7,8]. However, the slow rate of adsorption of commercially available activated alumina limits its use for treating large quantity of water. Many researchers have reported the potential of magnesium oxide

* Corresponding author. Tel.: +91 44 22574274; fax: +91 44 2254252.
E-mail address: ligy@iitm.ac.in (L. Philip).

1385-8947/$ – see front matter © 2007 Elsevier B.V. All rights reserved.
doi:10.1016/j.cej.2007.09.049

Nomenclature

C_e	equilibrium concentration of the adsorbate in the solution (mg l^{-1})
q_e	amount of adsorbate removed from aqueous solution at equilibrium (mg g^{-1})
q_t	amount of adsorbate sorbed on the adsorbent surface at any time t (mg g^{-1})
q_{cal}	calculated solid phase fluoride concentration at equilibrium (mg g^{-1})
q_{exp}	experimentally measured solid phase fluoride concentration at equilibrium (mg g^{-1})
k_1	first-order-rate constant of sorption (min^{-1})
k_2	second-order-rate constant of sorption (g mg^{-1} min^{-1})
K_p	constant of intraparticle diffusion (g mg^{-1} $min^{-1/2}$)
t	reaction time (min)
x	mass of solute adsorbed on the adsorbent (mg l^{-1})
m	mass of adsorbent (g l^{-1})
K_F	Freundlich isotherm constant (l g^{-1})
K_R	Redlich–Peterson isotherm constant (l g^{-1})
K_{RP}	Radke–Prausnitz isotherm constant (l g^{-1})
K_S	Sips isotherm constant (l g^{-1})
q_{mL}	monolayer capacity of Langmuir equation (mg g^{-1})
q_{mRP}	constant of Radke–Prausnitz isotherm
q_{mS}	specific sorption capacity of Sips equation at saturation (mg g^{-1})
q_{mT}	specific sorption capacity of Toth equation at saturation (mg g^{-1})
n	Freundlich adsorption intensity
b_L	Langmuir isotherm constant (l mg^{-1})
a_R	Redlich–Peterson isotherm constant (l mg^{-1})
A_T	Toth isotherm constant (l mg^{-1})
m_{RP}	Radke–Prausnitz isotherm model exponent
β	Redlich–Peterson isotherm model exponent
m_S	Sips isotherm model exponent
T	Toth isotherm model exponent

(magnesia) to scavenge fluoride [9–11]. However, magnesia is available only as fine powder. Employing metal oxides in powder forms as sorbent has practical limitations, including difficulty in solid/liquid separation, low hydraulic conductivity and leaching of the metal/metal-oxide along with treated water. To overcome the above-mentioned limitations, more environmental friendly and efficient techniques, which can be applicable to diverse end users, need to be developed.

In this paper, the defluoridation potential of a novel sorbent magnesia-amended activated alumina (MAAA) has been investigated in batch system. The physicochemical characteristics of MAAA were examined with XRD, SEM, EDAX and gas adsorption porosimetry analysis. Attempts have also been made to understand the adsorption kinetics, equilibrium and mechanism of adsorption.

2. Materials and methods

2.1. Sorbent preparations

MAAA was prepared by wet impregnation of commercially available AA (ACE Manufacturing and Marketing, AD-101F) with magnesium hydroxide slurry. For this, 1N NaOH solution was slowly added and mixed with 20 ml of magnesium chloride (4 M) solution until the pH rose up to ∼ 9.5. To this mixture, 20 g of AA particles (0.5–0.6 mm) were added, and allowed to settle for 30 min at room temperature. The samples were dried by evaporating excess water at 110 °C for 8 h with proper mixing and subsequently calcined at 450 °C for 2 h. Samples were then cooled to room temperature and washed with distilled water until the runoff was clear. These samples were then dried (150 °C for 8 h) and transferred to an airtight HDPE bottles for storage.

2.2. Sorbent characterization

The amount of magnesium coated on MAAA was quantified by acid digestion method suggested by national environment protection council [12]. Mineralogy of supported metal-oxide was characterized by powder XRD techniques (XD-D1, X-Ray Difractometer, Shimadzu, Japan). Crystalline phases of MAAA were identified by the software database published by the joint committee on power diffraction standards (JCPDS). Nitrogen chemisorption isotherm technique was used to measure specific surface area, pore-size distributions, and micropore volume of AA and MAAA using a micropore analyzer (ASAP 2020, Micromeritics, USA). The analysis bath temperature was −195.779 °C. PHzpc (pH of point of zero charge) of MAAA were determined by batch equilibrium method [13]. Surface morphology and spot elemental analysis of MAAA was carried out using SEM and EDAX, respectively (FEI, Quanta 200, Czechoslovakia).

2.3. Batch sorption experiments

All batch fluoride sorption studies were carried out in 250 ml Teflon flasks with a working volume of 100 ml. After adding the required quantity of the sorbent to the fluoride-spiked solution, the flasks were kept in an orbital shaker with thermostatic control (Remi, India) at 90 rpm and 30 ± 1 °C for specified contact time. Once the sorption equilibrium was reached (180 min), the liquid samples were collected and analyzed for residual fluoride concentration using ion chromatography (Dionex, LC-20 chromatography, AD-25 absorbance detector, USA). The concentrations of free metal ions in solutions were also measured using atomic absorption spectrometer (AAS, GBC 932 Plus, Australia). The initial pH of the fluoride solution was maintained between 6.5 and 7 by using dilute NaOH or HCl solutions.

The effect of contact time on fluoride sorption was investigated by adding a 4 g l^{-1} of MAAA into 100 ml fluoride-spiked solution of various fluoride concentrations (∼5, 10, 20 and 30 mg/l). The liquid samples were withdrawn at pre-determined time intervals and analyzed for residual fluoride concentrations.

Equilibrium sorption studies were conducted at 30 ± 1 °C, with varying fluoride concentrations (~5–150 mg l^{-1}).

Sorption experiments were also carried out at various pHs (2–10) to understand the effect of pH on fluoride sorption. The solution pH was adjusted by adding different dilutions of HCl and NaOH solutions. The pH measurements were carried out with ion analyzer connected with pH electrode (Expandable Ion Analyzer, USA).

2.3.1. Effect of other co-existing ions

The interference effect of different ions usually present in real ground water sample on fluoride sorption by MAAA was also studied. Various concentrations of ions, including Cl^-, NO_3^-, SO_4^{2-}, HCO_3^-, SiO_3^-, PO_4^{3-}, humic acid, and Ca^{2+} were spiked with 10 mg l^{-1} of fluoride solution. Adsorption studies were carried out as described earlier with an adsorbent dose of 4 g l^{-1}.The liquid sample were withdrawn after 3 h, filtered and analyzed for residual fluoride concentrations.

2.3.2. Regeneration experiments

To test the regeneration capacity of the adsorbent, studies were carried out with various concentrations of NaOH (0.0–2%) as eluent. For this, initial adsorption study was conducted using 4 g l^{-1} MAAA and ~5 mg l^{-1} of fluoride solution. The sorbent was then separated by means of filtration and washed with distilled water to remove liquid containing fluoride. The adsorbed fluoride was then eluted with various concentrations of NaOH and the eluent was separated and analyzed for fluoride concentrations.

3. Results and discussion

3.1. Sorbent characterization

The MAAA prepared as discussed earlier was characterized by powder XRD. Fig. 1 shows the X-ray diffraction pattern of MAAA. Analyzing the X-ray pattern using the software database published by the JCPDS; it was found that all the peaks observed in the X-ray diffraction pattern was best suiting the alumina ($Al_{21.333}O_{32}$, JCPDS – 80-0955). No peaks that correspond to magnesia and other forms of magnesium were found. This may be due to the amorphous nature of the magnesia or small volume of magnesia compared to AA. The magnesium content on the MAAA was found to be 44–50 mg g^{-1}. The surface characteristics of both AA and MAAA were determined by nitrogen chemisorption technique (Table 1). Fig. 2 shows SEM micrograms taken at 10,000× and 5000× magnification to observe

Table 1
Physical characteristics of AA and MAAA

Physical characteristics	AA	MAAA
BET surface area	242.07 m^2 g^{-1}	193.5 m^2 g^{-1}
BJH adsorption cumulative volume of pores between 17.000 and 3000.000 Å diameter	0.299 cm^3 g^{-1}	0.252 cm^3 g^{-1}
BJH desorption cumulative volume of pores between 17.000 and 3000.000 Å diameter	0.306 cm^3 g^{-1}	0.286 cm^3 g^{-1}
Adsorption average pore width (4V/A by BET)	5.57 nm	5.69 nm
BJH adsorption average pore diameter (4V/A)	5.65 nm	5.57 nm
BJH desorption average pore diameter (4V/A)	5.97 nm	4.74 nm

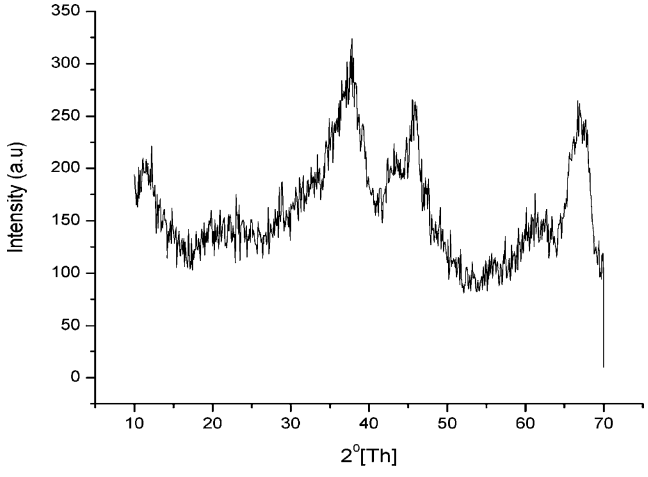

Fig. 1. X-Ray diffraction pattern of magnesia-amended activated alumina.

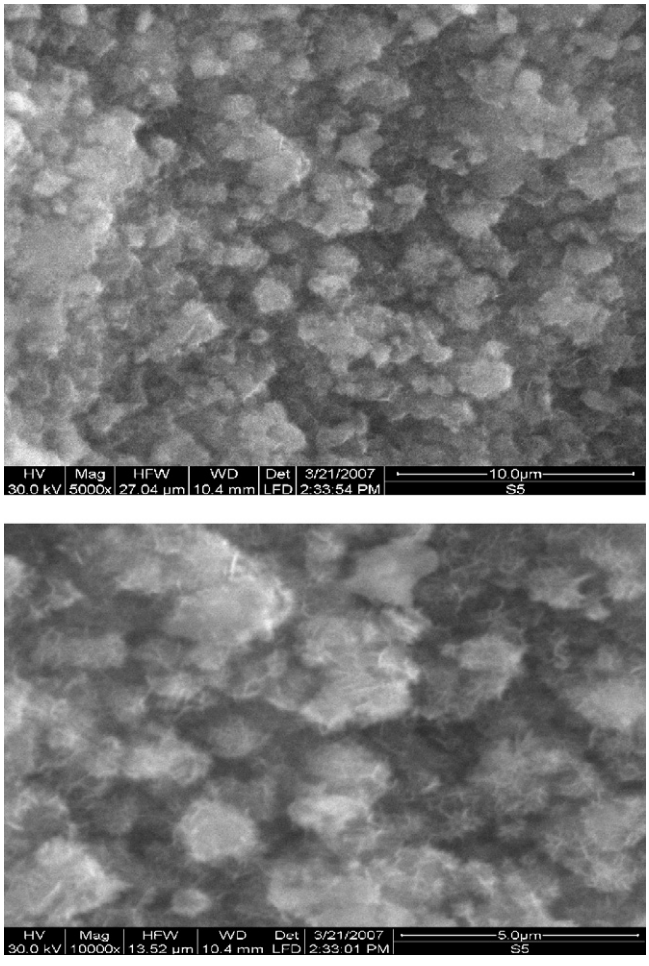

Fig. 2. SEM micrograph of magnesia-amended activated alumina.

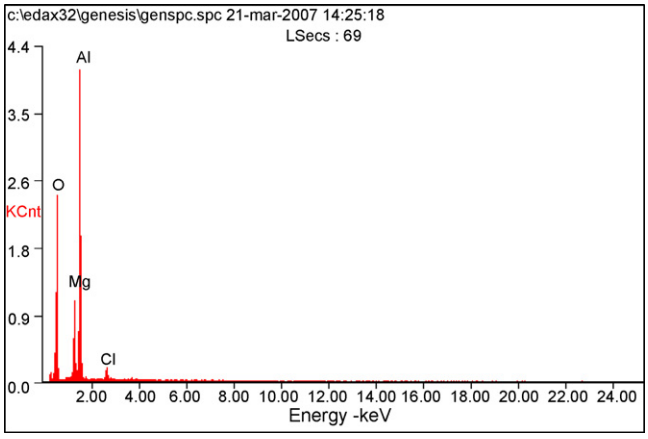

Fig. 3. EDAX spectrum of magnesia-amended activated alumina.

the surface morphology of MAAA. The spot elemental analysis of MAAA was done by EDAX technique. The EDAX spectrum (Fig. 3) shows the signals corresponding to Al, Mg, and O, which shows an indirect evidence for magnesia on the surface of AA.

Zero point of charge (pHzpc) is a tool to determine under what pH the MAAA surface has positive or negative surface charge. F^- like anions is strongly adsorbed when the pHzpc relationship causes the material surface to be positive. The pHzpc MAAA determined by simple batch equilibrium method using NaCl (0.1 and 0.01 M) as background electrolyte was found to be 8.6 ± 0.2, which is slightly higher than the pHzpc value obtained for AA (8.25 ± 0.2). Insignificant variations in pHzpc value with respect to the variations in background electrolyte concentrations, indicate that NaCl is an indifferent electrolyte and pHzpc is independent of its concentration. The pHzpc obtained for MAAA is difficult to compare with other literature values, as this is the first time such material is developed in lab. Different pHzpc values ranging from 5 to 9 were reported for aluminium-based oxides/hydroxide in the literatures. These values were obtained by different methods by different investigators, and these numbers are not necessarily comparable [14].

3.2. Effect of initial concentration and contact time

The kinetics of sorption is an important parameter for designing sorption system and is required for selecting optimum operating conditions for full-scale batch process [15]. Fig. 4 illustrates the kinetics of fluoride sorption onto MAAA at various initial concentrations. For all the initial fluoride concentrations studied, most of the removal took place during the first 60 min and the system reached a pseudo-equilibrium value slowly in 180 min. No appreciable removal was noticed with higher contact time. This indicates that initial concentration of fluoride has least effect on equilibrium time. From the shape of the kinetic curves (Fig. 4), it is also evident that the fluoride sorption onto MAAA is a two-step process, i.e. initial rapid adsorption during the first 60 min and slow rate of sorption until the equilibrium is reached. For an initial concentration of 30 mg l^{-1} of fluoride, ~72% of the removal took place in first 60 min and reached pseudo equilibrium in 180 min with a further ~8% increase in sorption.

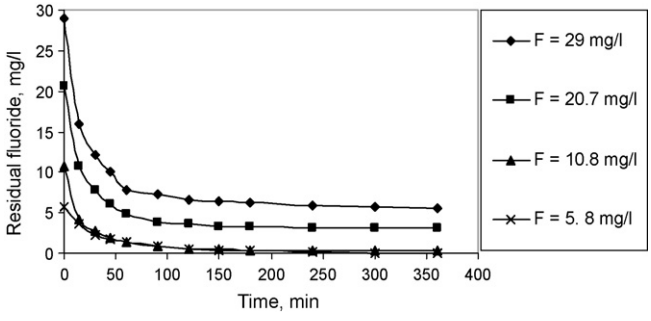

Fig. 4. Kinetics of fluoride removal by MAAA at various initial concentrations of fluoride (adsorbent dose = 4 g l^{-1}).

The kinetics of any sorption process is a function of different parameters, such as the structural properties of sorbent, nature and concentration of sorbate, and sorbent–sorbate interactions. To understand the dynamics of solute adsorption process, fluoride sorption kinetic data were analyzed using two mass transfer and one intraparticle diffusion models. These models are pseudo first-order equation [16], pseudo-second-order equation [17] and intraparticle diffusion model [18]. The mathematical representations (nonlinear) of these models are as follows:

Pseudo-first-order equation : $$q_t = q_e(1 - e^{-k_1 t})$$

Pseudo- second-order equation : $$q_t = \frac{q_e^2 k_2 t}{1 + q_e k_2 t}$$

Intraparticle diffusion model : $$q_t = k_p t^{1/2}$$

Linear regressions methods are the commonly used technique for determining the best-fitting kinetic models. Many researches have shown that it is not appropriate to use the linear regression method for comparing the best fitting of kinetic model [19,20]. Non-linear methods are better way to obtain the kinetic parameters. In our study, non-linear method was used to find the best-fitting model and kinetic parameters, which were found by trial and error method by means of Microsoft's spreadsheet, Excel® software package using *solver* add-in option. To find out the best fit, the root mean squared error (RMSE) was found out using the following equation:

$$\text{RMSE} = \sqrt{\frac{1}{n}\sum_{i=1}^{N}(q_{\text{cal}_i} - q_{\text{exp}_i})^2}$$

where q_{cal} and q_{exp} represent the predicted and measured value of solid phase fluoride concentrations at equilibrium. Figs. 5 and 6 show the pseudo-first-order- and second-order-equation plots for adsorption of fluoride onto MAAA. The adsorption kinetic model parameters obtained from the above plots are given in Table 2. The kinetic rate coefficient obtained was found to be a function of initial fluoride concentration. A direct relationship was observed between kinetic rate and initial fluoride concentration. Many sorption studies using metal oxide conducted by previous researchers have observed an increasing trend in reaction rate at higher concentration of fluoride [7,8].

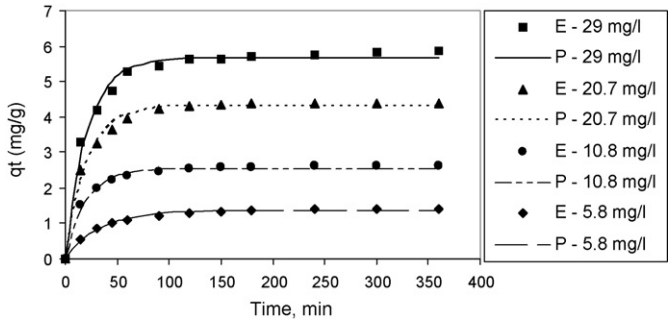

Fig. 5. Pseudo-first-order kinetic plots for the sorption of fluoride onto MAAA at various initial concentrations (E – experimental; P – predicted).

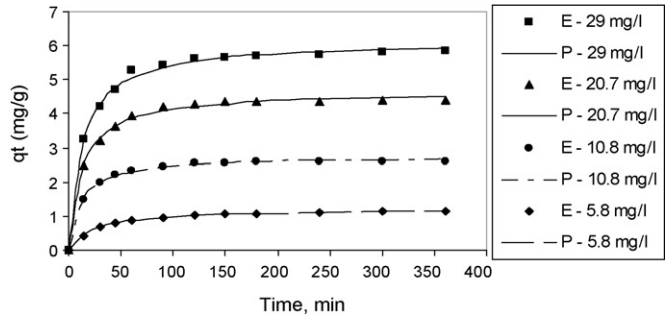

Fig. 6. Pseudo-second-order kinetic plots for the sorption of fluoride onto MAAA at various initial concentrations (E – experimental; P – predicted).

From Table 2, it is also clear that kinetic data fitted well with pseudo-second-order equation, which is evident from the less RMSE value. This also indicates that adsorption mechanism of fluoride onto MAAA might be a chemisorption process.

The possible reaction mechanism for adsorption of fluoride onto MAAA can be hypothesized as below. In aqueous solution, the coated magnesia hydrates to $Mg(OH)_2$ according to the reaction:

$$MgO + H_2O \rightarrow Mg(OH)_2\ [\text{brucite}] \quad (R1)$$

During the formation of magnesium hydroxide, the fluoride ions present in the contaminated water replace the hydroxyl ions of brucite crystal lattice without disturbing the crystal structure of the compound. Such substitution is possible because F^- and OH^- ions are of similar size with comparable ionic radius; also, they are iso-electronic in nature. This kind of substitution is generally termed as isomorphous substitution.

$$Mg(OH)_2 + F^- \leftrightarrow Mg(OH)_{2-y}F_y \quad (R2)$$

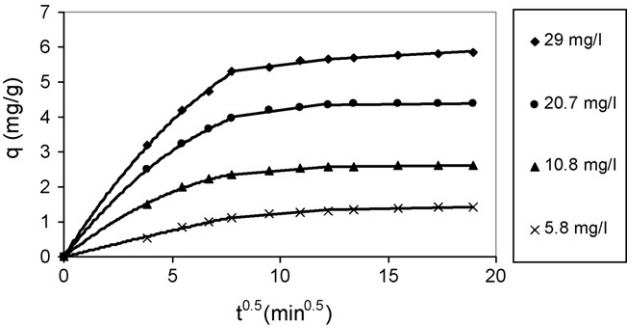

Fig. 7. Intraparticle mass transfer curves for sorption of fluoride onto MAAA.

Generally, adsorption onto a solid surface is considered as a surface phenomenon. However, the possibility of intraparticle diffusion into porous adsorbent cannot be neglected. Allen et al. [21] reported that for any porous materials, especially in an agitated system, the main resistance to mass transfer occurs during the movement or diffusion of solute within the pores of the particles. Axe and Trivedi [22] found that intraparticle surface diffusion was the rate-limiting process for metal ion adsorption by micro-porous metal oxides in aquatic and soil environment. To understand the contribution of intraparticle diffusion in fluoride sorption process onto MAAA, kinetic data were fitted with Weber–Morris intraparticle diffusion model [18]. Fig. 7 shows the intraparticle mass transfer curves at various fluoride concentrations. In most cases, q_t vs. $t^{1/2}$ plots will give general features of three distinct phases. The first phase (initial curved portion) is generally due to external surface sorption, the intermediate linear portion is due to intraparticle diffusion and the final plateau is due to equilibrium sorption. From Fig. 7, it is clear that intraparticle diffusion is slow. The intraparticle diffusion coefficient (K_p), values were calculated from the slope of a linear plot of q_t against square root of time ($t^{1/2}$). The calculated (K_p), were found to be 0.083, 0.086, 0.054 and 00.049 g mg^{-1} min$^{-1/2}$ at initial fluoride concentrations of 29, 20.7, 10.8 and 5.8 mg l^{-1}, respectively. However, the linear portion of the curves did not pass through the origin, which indicates the complex nature of the adsorption process. From this observation, it may be concluded that fluoride sorption onto MAAA is a complex process and both intraparticle diffusion and surface sorption contributes to the rate-limiting step.

3.3. Adsorption isotherms

Analysis of isotherm data is important for predicting the adsorption capacity of the sorbent, which is one of the main

Table 2
Pseudo-first-order and pseudo-second-order-rate parameters obtained for the sorption of fluoride on MAAA

Fluoride concentration (mg/l)	First-order-rate parameters			Second-order-rate parameters		
	k_1 (l min^{-1})	q_e (mg g^{-1})	RMSE	k_2 (g mg^{-1} min^{-1})	q_e (mg g^{-1})	RMSE
29	0.0474	5.673	0.151	0.0127	6.126	0.084
20.7	0.0484	4.318	0.108	0.0174	4.649	0.0559
10.8	0.0514	2.560	0.060	0.0315	2.751	0.0228
5.8	0.0299	1.366	0.033	0.0330	1.22	0.0108

Table 3
Two and three parameter isotherm models used in this study

Isotherm models	Mathematical expressions	Model parameters
Langmuir (L)	$q_e = \frac{q_L b_L C_e}{1+b_L C_e}$	$q_{L\ (mg\,g^{-1})}$, b_L ($l\,mg^{-1}$)
Freundlich (F)	$q_e = K_F C_e^{1/n}$	K_F ($l\,g^{-1}$), $1/n$
Redlich–Peterson (R)	$q_e = \frac{K_R C_e}{1+a_R C_e^{\beta}}$	K_R ($l\,g^{-1}$), a_R ($l\,mg^{-1}$), β
Radke–Prausnitz (RP)	$q_e = \frac{K_{RP} q_{mRP} C_e}{(1+K_{RP} C_e)^{m_{RP}}}$	K_{RP} ($l\,g^{-1}$), q_{mRP}, m_{RP}
Sips (S)	$q_e = \frac{q_{ms}(K_s C_e)^{m_s}}{(1+K_s C_e)^{m_s}}$	K_S ($l\,g^{-1}$), q_{ms} ($mg\,g^{-1}$), m_S
Toth (T)	$q_e = \frac{q_{mT} C_e}{(A_T + C_e^T)^{1/T}}$	q_{mT} ($mg\,g^{-1}$), A_T ($l\,mg^{-1}$), T

parameter required for the design of an adsorption system. Several isotherm model equations have been used for this purpose. The mathematical expressions of some of them, used in this study, are summarized in Table 3. The details of the isotherms listed in the Table 4 are available in various literatures [23–28].

Where q_e is the amount of solute adsorbed per weight of adsorbent at equilibrium ($mg\,g^{-1}$); C_e is equilibrium concentration of the adsorbate in the solution ($mg\,l^{-1}$); K_F, K_R, K_{RP}, and K_S are the Freundlich, Redlich–Peterson; Radke–Prausnitz, and Sips constants, respectively. q_L, q_{mRP}, q_{ms}, and q_{mT} represent maximum specific uptake capacity at equilibrium; b_L, a_R a_{LF} and A_T are affinity coefficients ($l\,mg^{-1}$). $1/n$, β, and T are heterogeneity coefficients.

Among these models, Langmuir (L) and Freundlich (F) belong to 'two constant' models and other listed isotherm models falls into 'three constant' models. Figs. 8 and 9 depicts the different adsorption isotherms model plots along with experimental data (initial fluoride concentrations range ~5–150 $mg\,l^{-1}$) for MAAA and AA, respectively. The estimated isotherm parameters obtained from these model fits are given in Tables 4 (MAAA) and 5 (AA). L and F, the two most widely used isotherm models, did not represent the equilibrium data well, which is evident from the high RMSE value. L model is an analytical equation that assumes monolayer coverage of adsorbate over a homogenous adsorbent surface [23]. This model does not consider surface heterogeneity of the sorbent. It assumes fluoride sorption will take place only at specific sorption sites within the sorbent. The F model is an empirical equation that considers the surface heterogeneity of the sorbent, developed for liquid phase adsorption [24]. However, no improvement in model performance was observed by considering the surface heterogeneity factor. Freundlich expression is an exponential equation and therefore, theoretically, an infinite amount of sorption can occur using this equation. However,

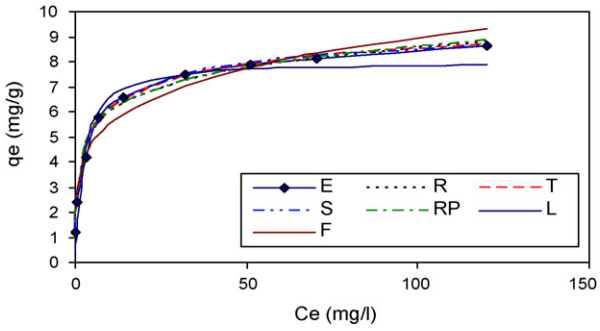

Fig. 8. Isotherm plots obtained from various isotherm models (adsorbent = MAAA, adsorbent dose = 4 $g\,l^{-1}$, initial pH 6.5–7; F^- concentration range, 5–150 $mg\,l^{-1}$) (E – experimental; R – Redlich–Peterson; RP – Radke–Prausnitz; S – Sips; T – Toth).

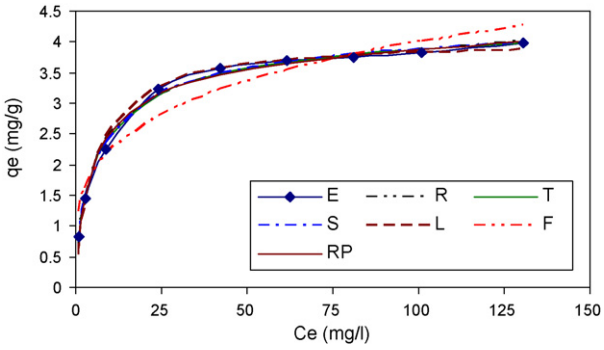

Fig. 9. Isotherm plots obtained from various isotherm models (adsorbent = AA, adsorbent dose = 4 $g\,l^{-1}$, initial pH 6-5-7; F^- concentration range, 5–150 $mg\,l^{-1}$) (E – experimental; R – Redlich–Peterson; RP – Radke–Prausnitz; S – Sips; T – Toth).

the experimental evidence indicates that an isotherm plateau is reached at a limiting value of the solid phase concentration. This plateau is not predicted by the F isotherm, which indicates that the equation itself does not have any real physical significance. Mckay [29] reported that both L and F theories could not predict the equilibrium data over wide concentration range.

Among the three parameter model tested, Sips (S) model predicted equilibrium data well (RMSE = 0.156) followed by Toth (T) model (RMSE = 0.176). S model is a combination of L and F models having features of both L and F equations. Toth model is an improved version of S model, which is derived from potential theory and is applicable for heterogeneous equations [28]. It assumes that, most sites have adsorption energy lower than the peak or maximum adsorption energy. However, no improvement in equilibrium data prediction was observed. The Redlich–Peterson (R) [25] and Radke–Prausnitz (RP) [26]

Table 4
Isotherm parameters obtained by fitting equilibrium data (for sorption of fluoride onto MAAA) with various isotherm models

Isotherm models	Frendlich	Langmuir	Radke-prausmitz	Redlich–Peterson	Sips	Toth
Isotherm parameters	$K_F = 3.36$ $1/n = 0.214$ –	$q_{mL} = 8.08$ $b = 0.416$ –	$K_{RP} = 2.620$ $q_{mRP} = 3.852$ $m_{RP} = 0.854$	$K_R = 12.05$ $a_R = 3.098$ $\beta = 0.861$	$K_S = 0.211$ $q_{ms} = 10.12$ $m_S = 0.542$	$A_T = 0.609$ $q_{mT} = 11.38$ $T = 0.367$
RMSE	0.564	0.560	0.277	0.262	0.156	0.176

Table 5
Isotherm parameters obtained by fitting equilibrium data (for sorption of fluoride onto AA) with various isotherm models

Isotherm models	Frendlich	Langmuir	Radke-prausmitz	Redlich–Peterson	Sips	Toth
Isotherm parameters	$K_F = 1.268$ $n = 4.07$ –	$q_{mL} = 4.04$ $b = 0.177$ –	$K_{RP} = 0.308$ $q_{mRP} = 2.97$ $m_{RP} = 0.91$	$K_R = 1.07$ $a_R = 0.33$ $\beta = 0.92$	$K_S = 0.135$ $q_{ms} = 4.43$ $m_S = 0.74$	$A_T = 2.039$ $q_{mT} = 4.58$ $T = 0.63$
RMSE	0.271	0.128	0.101	0.096	0.0.068	0.077

models also predicted equilibrium date well compared to L and F models. However, the performances of these models are below S and T model equations. The estimated fluoride sorption capacity of MAAA (Table 4) was found to be much higher than the base material AA (Table 5). In recent years, many other sorbents have been investigated for the removal of fluoride from water systems [7,8,30–38]. While comparing the fluoride sorption potential of most of the sorbents reported in the recent literatures, MAAA is found to be highly competitive. Tripathy and co-workers has reported a high adsorption capacity for alum impregnated activated alumina (AIAA) [34]. However, it is important to note that the theoretical/predicted adsorption capacity (40.3 mg g^{-1}) of AIAA is much higher than the actual (experimental) adsorption capacity of the sorbent. This may be mainly due to the wide variations of the experimental parameters, especially initial fluoride concentrations range adopted in the equilibrium sorption experiments. Das et al has also reported a similar kind of observation [8].

3.4. Effect of pH

In most of the solid/liquid sorption process, the solution pH has great importance in deciding the sorption potential of the sorbent. Fig. 10 shows the fluoride uptake capacity of MAAA at various pH values (range 2–10). From Fig. 10, it is observed that a positive shift in the final solution pH was observed from the initial set pH value, after 3 h of adsorption, in the acidic range. However, a negative shift in the final solution pH was observed in the case when initial pH was in basic range (9–10). By looking at the initial and final pH values, the optimum removal took place between pH 6 and 7.5. A progressive decrease in fluoride removal was observed with increase in pH. This may be mainly attributed to the competition for the active sites by OH^- ions

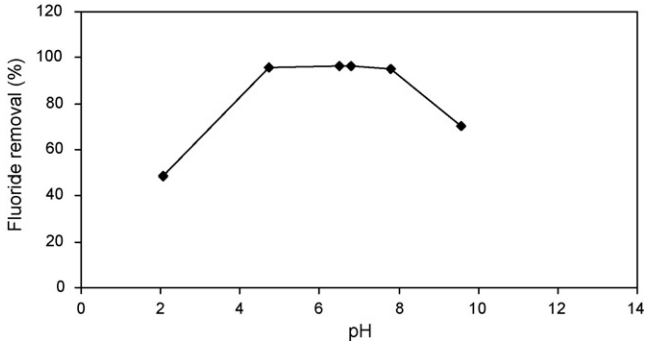

Fig. 10. Effect of solution pH on fluoride removal by MAAA (initial fluoride concentration = ~ 10 mg l^{-1}, adsorbent dose = 4 g l^{-1}).

and the electrostatic repulsion of fluoride ions by the negatively charged MAAA surface. Below pH 8.6 (pHzpc), the decreased fluoride removal observed may be due to the competition for the active sites by hydroxyl ions. Since the MAAA surface has a net positive charge at pH below 8.6 (pHzpc = 8.6 ± 0.2), the chance of electrostatic repulsion can be ruled out. However, the reduction in fluoride removal capacity at higher alkaline pH ranges (above pHzpc) can be attributed to the electrostatic repulsion from the negatively charged MAAA surface. The less removal capacity in acidic pH may be attributed to the formation of weak HF ions [39] or may due to the complexation of F^- ions with dissolved aluminum.

3.5. Effect of co-existing ions

The contaminated ground water contains several other co-existing ions along with fluoride, which may compete with fluoride for the active sorption sites. However, the investigations conducted so far are with distilled water spiked with fluoride, where the concentration of other ions present is negligible. Hence, it is important to investigate the interference of co-existing ions on fluoride sorption onto MAAA for evaluating the suitability of MAAA for field applications. Figs. 11a–c show the effect of various co-existing ions of different concentrations on fluoride sorption by MAAA. Except SO_4^{2-} and HCO_3^-, all other co-existing ions (Cl^-, NO_3^-, SiO_3^-, PO_4^{3-}, humic acid, and Ca^{2+}) have shown negligible effect on fluoride sorption. Interference was observed on fluoride sorption by SO_4^{2-} ions above a concentration of 50 mg l^{-1}. Fluoride sorption capacity was reduced by ~20–25% for an initial SO_4^{2-} concentration of 200 mg l^{-1}. HCO_3^- has also shown a negative shift in fluoride sorption by a value of ~10% for an initial concentration of 200 mg l^{-1}. Compared to other ions, addition of SO_4^{2-} and HCO_3^- ions have shown more shift in pH. Addition of these ions increased the pH to 8.4 ± 0.2 and 8.8 ± 0.2, respectively. However, in the cases when no ions were present and when ions like Cl^-, NO_3^-, SiO_3^-, PO_4^{3-}, and humic acid were present, increase in pH observed (7.6–8) was comparable. The reduction in fluoride removal observed by the presence of SO_4^{2-} and HCO_3^- may be due to competition from these ions for active sorption site or due to the change in pH or combination of these two. Detailed studies are required to elucidate the exact reason.

3.6. Regeneration studies

Regenerabilty of any exhausted sorbent is a crucial factor in any sorption process for improving the process economics.

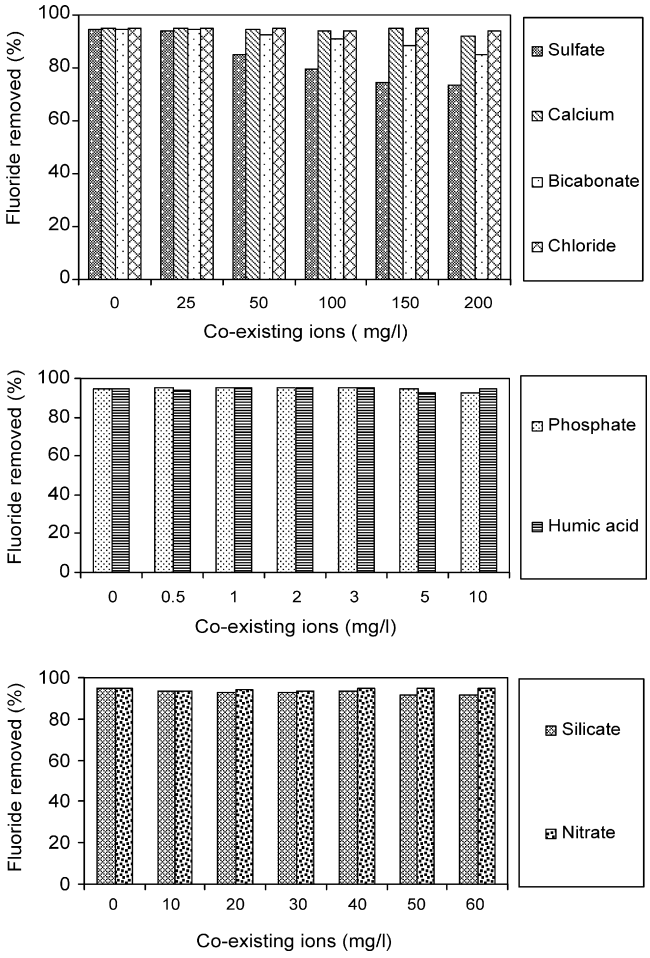

Fig. 11. (a–c) Individual effect of different co-existing ions on fluoride sorption by MAAA ((initial fluoride concentration = ~10 mg l^{-1}, adsorbent dose = 4 g l^{-1}).

In this study, various concentrations of NaOH were used as an eluent to check its eluting potential (Fig. 12). From this study, it was observed that 2% NaOH could elute nearly ~90% adsorbed fluoride from MAAA.

In order to check the reusability of MAAA, it was subjected to successive adsorption–desorption cycles. The results of these studies (Fig. 13) showed that a considerable reduction in adsorption efficiency occurred in the second and third cycles

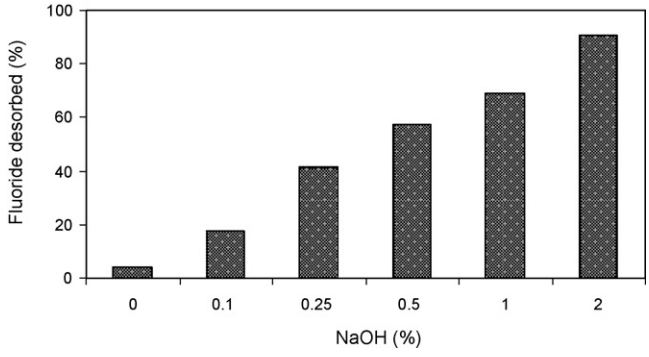

Fig. 12. Fluoride eluted at various concentration of sodium hydroxide (initial fluoride concentration = 5 mg l^{-1}, adsorbent dose = 4 g l^{-1}, contact time = 1 h).

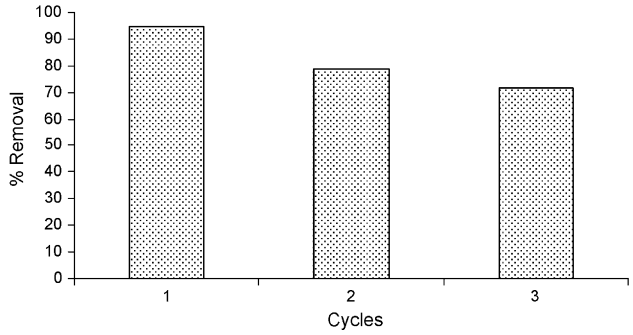

Fig. 13. Performance of MAAA after regeneration by NaOH (initial fluoride concentration = 10.4 mg l^{-1}).

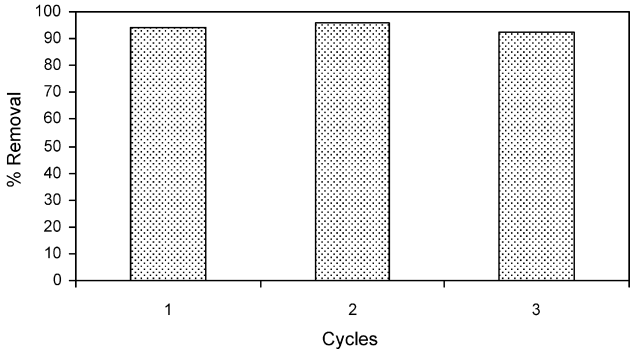

Fig. 14. Performance of MAAA after regeneration and recoating with MgO (initial fluoride concentration = 10.4 mg l^{-1}).

of adsorption after the regeneration. At the end of third cycle, ~20% reduction in efficiency was observed. This reduction in adsorption efficiency may be attributed to the gradual dissolution of magnesium from the MAAA surface during vigorous washing of the sorbent, after soaking it in 2% NaOH solution, to bring the pH to neutral (solubility of magnesia = 0.0006 g in 100 ml). The amount of magnesium estimated on the surface of MAAA at the end of third cycles was 11.2 mg g^{-1} whereas initially it was 40–50 mg g^{-1}. Hence, a new regeneration protocol was developed by recoating the sorbent before each cycle of adsorption. For this, after desorption process using NaOH, sorbents were dipped in 4 M magnesium nitrate solution for 2–3 h and the excess magnesium nitrate was poured off. This mixture were dried and claimed at 450 °C and used for next adsorption cycle. Fig. 14 shows the adsorption efficiency of MAAA after recoating with magnesia. As evident form the Fig. 14 there was no reduction in adsorption efficacy upto 3rd cycle.

4. Conclusions

In this study, a novel sorbent, magnesia-amended alumina has been prepared and examined for its potential in removing fluoride from drinking water system. This material has shown much higher and faster fluoride removal compared to AA. The main conclusions drawn from the present study are:

- Among different factors tested, pH is found to be the most influential factor for fluoride uptake by MAAA. An optimum fluoride removal was observed in the pH range of 5–7.5. This pH range is very reasonable in real situations.
- Most of the common interfering ions have shown insignificant effect on fluoride sorption by MAAA. This shows the adsorbent's high fluoride selectivity and suitability in practical situations.
- Fluoride sorption was very rapid during the first 60 min and there after slowly reached the pseudo-equilibrium value in 3 h, Adsorption kinetics followed pseudo-second-order model, which indicates that F^- removal might be due to chemisorption process. The rate of sorption by MAAA was much higher than that of AA. Fluoride uptake by MAAA is a complex process. Both surface sorption as well as intraparticle diffusion plays a significant role in the sorption process.
- Two parameter isotherm models (L and F) could not predict the equilibrium data well, whereas three parameter isotherm models such as Sips and Toth represented equilibrium data well with least RMSE. The predicted fluoride adsorption capacity of MAAA was found to be much higher than AA and many other commonly used sorbents.
- The fluoride bearing MAAA could be regenerated easily with 2% sodium hydroxide solution as eluent.

Appendix A. Supplementary data

Supplementary data associated with this article can be found, in the online version, at doi:10.1016/j.cej.2007.09.049.

References

[1] T. Tsutsui, N. Suzuki, M. Ohmori, H. Maizumi, Cytotoxicity, chromosome aberrations and unscheduled DNA synthesis in cultured human diploid fibroblasts induced by sodium fluoride, Mutat. Res. Apr. 139 (4) (1984) 193–198.

[2] A.G. Wang, T. Xia, Q.L. Chu, M. Zhang, F. Liu, X.M. Chen, K.D. Yang, Effects of fluoride on lipid peroxidation, DNA damage and apoptosis in human embryohepatocytes, Biomed. Environ. Sci. 17 (2) (2004) 217–222.

[3] WHO, Guidelines for drinking-water quality first addendum to third edition, Volume 1 recommandations, 2006 (http://www.who.int/water_sanitation_health/dwq/gdwq0506.pdf).

[4] S. Maurice, O.Y. Kojima, O. Aoyi, C. Eileen, B.H. Matsuda, Adsorption equilibrium modeling and solution chemistry dependence of fluoride removal from water by trivalent-cation-exchanged zeolite F-9, J. Colloid.Interface Sci. 279 (2004) 341–350.

[5] S.M. Maliyekkal, A.K. Sharma, L. Philip, Manganese-oxide-coated alumina: a promising sorbent for defluoridation of water, Water Res. 40 (19) (2006) 3497–3506.

[6] R.C. Meenakshi, Maheshwary, Fluoride in drinking water and its removal, J. Hazard. Mater. 137 (1) (2006) 456–463.

[7] S. Ghorai, K.K. Pant, Equilibrium, kinetics and breakthrough studies for adsorption of fluoride on activated alumina, Sep. Purif. Technol. 42 (2005) 265–271.

[8] N. Das, P. Pattanaik, R. Das, Defluoridation of drinking water using activated titanium rich bauxite, J. Colloid.Interface Sci. 292 (2005) 1–10.

[9] A.C. Zettlemoyer, E.A. Zettlemoyer, W.C. Walker, Active magnesia II: adsorption of fluoride from aqueous solution, J. Am. Chem. Soc. 69 (1947) 1312–1315.

[10] P. Venkateswarlu, D.N. Rao, Investigation on the fluoride removal from water: rapid removal of fluoride with magnesium oxide, Ind. J. Med. Res. 41 (1953) 473–477.

[11] S.M. Rao, P. Mamatha, Water quality in sustainable water management, Curr. Sci. 87 (2004) 942–947.

[12] National Environment Protection Council (NEPC), Guideline on laboratory analysis of potentially contaminated soils, Schedule B (3) (1999) (http://www.ephc.gov.au/pdf/cs/cs_03_lab_analysis.pdf).

[13] B.M. Babic, S.K. Milonjic, M.J. Polovina, B.V. Kaludierovic, Point of zero charge and intrinsic equilibrium constants of activated carbon cloth, Carbon 37 (1999) 477–481.

[14] J. Hlavay, K. Polyák, Determination of surface properties of iron hydroxide-coated alumina adsorbent prepared for removal of arsenic from drinking water, J. Colloid Interface Sci. 284 (1) (2005) 71–77.

[15] E.A. Oliveira, S.F. Montanher, A.D. Andrade, J.A. Nóbrega, M.C. Rollemberg, Equilibrium studies for the sorption of chromium and nickel from aqueous solutions using raw rice bran, Process Biochem. 40 (2005) 3485–3490.

[16] S. Lagergren, Zur theorie der sogenannten adsorption gelöster stoffe, K. Sven, Vetenskapsakad Handl. 24 (1898) 1–39.

[17] Y.S. Ho, G. McKay, The kinetics of sorption of divalent metal ions onto sphagnum moss peat, Water Res. 34 (2000) 735–742.

[18] W.J. Weber Jr., J.C. Morris, Kinetics of adsorption on carbon from solution, J. Sanit. Eng. Div. ASCE 89 (1963) 31–59.

[19] Y.S. Ho, Second-order kinetic model for the sorption of cadmium onto tree fern: a comparison of linear and non-linear methods, Water Res. 40 (1) (2006) 119–125.

[20] K.V. Kumar, Comparative analysis of linear and non-linear method of estimating the sorption isotherm parameters for malachite green onto activated carbon, J. Hazard. Mater. 136 (2) (2006) 197–202.

[21] S.J. Allen, G. McKay, K.Y.H. Khader, Intraparticle diffusion of a basic dye during adsorption onto sphagnum peat, Environ. Pollut. 56 (1989) 39–50.

[22] L. Axe, P. Trivedi, Intraparticle surface diffusion of metal contaminants and their attenuation in microporous amorphous Al, Fe, and Mn oxides, J. Colloid Interface Sci. 247 (2) (2002) 259–265.

[23] I. Langmuir, The adsorption of gases on plane surface of glass, mica and platinum, J. Am. Chem. Soc. 40 (1916) 1361–1403.

[24] H.M.F. Freundlich, Über die adsorption in Lösungen, Z. Phys. Chem. 57 (1906) 385–470.

[25] O. Redlich, C. Peterson, Useful adsorption isotherm, J. Phys. Chem. 63 (1958) 1024.

[26] C.J. Radke, J.M. Prausnitz, Adsorption of organic solutes from dilute aqueous solutions on activated carbon, Ind. Eng. Chem. Fundam. 11 (1972) 445–450.

[27] R. Sips, Structure of a catalyst surface, J. Chem. Phys. 16 (1948) 490–495.

[28] J. Toth, State equations of the solid gas interface layer, Acta Chem. Acad. Hung. 69 (1971) 311–317.

[29] G. McKay, Kinetics of colour removal from effluent using activated carbon, JSDC 96 (1980) 576–579.

[30] S. Ayoob, A.K. Gupta, Sorptive response profile of an adsorbent in the defluoridation of drinking water, Chem. Eng. J. 133 (1–3) (2007) 273–281.

[31] H. Wang, J. Chen, Y. Cai, J. Ji, L. Liu, H.H. Teng, Defluoridation of drinking water by Mg/Al hydrotalcite-like compounds and their calcined products, Appl. Clay Sci. 35 (2007) 59–66.

[32] S.P. Kamble, S. Jagtap, K.N. Labhsetwar, D. Thakare, S. Godfrey, S. Devotta, S.S. Rayalu, Defluoridation of drinking water using chitin, chitosan and lanthanum-modified chitosan, Chem. Eng. J. 129 (1–3) (2007) 173–180.

[33] M. Sarkar, A. Banerjee, P.P. Pramanick, A.R. Sarkar, Use of laterite for the removal of fluoride from contaminated drinking water, J. Colloid Interface Sci. 302 (2) (2006) 432–441.

[34] S.S. Tripathy, J.L. Bersillon, K. Gopal, Removal of fluoride from drinking water by adsorption onto alum-impregnated activated alumina, Sep. Purif. Technol. 50 (3) (2006) 310–317.

[35] M. Islam, R.K. Patel, Evaluation of removal efficiency of fluoride from aqueous solution using quick lime, J. Hazard. Mater. 143 (1–2) (2007) 303–310.

[36] E. Oguz, Equilibrium isotherms and kinetics studies for the sorption of fluoride on light weight concrete materials, Colloids Surf. A: Physicochem. Eng. Aspects 295 (1–3) (2007) 258–263.
[37] V. Gopal, K.P. Elango, Equilibrium, kinetic and thermodynamic studies of adsorption of fluoride onto plaster of Paris, J. Hazard. Mater. 141 (1) (2007) 98–105.
[38] M. Mahramanlioglu, I. Kizilcikli, I.O. Bicer, Adsorption of fluoride from aqueous solution by acid treated spent bleaching earth, J. Fluorine Chem. 115 (2002) 41–47.
[39] A.M. Raichur, M.J. Basu, Adsorption of fluoride onto mixed rare earth oxides, Sep. Purif. Technol. 24 (2001) 121–127.